THE COMPANY OF **Biologists**

RESEARCH ARTICLE

Hemolymph circulation in insect sensory appendages: functional mechanics of antennal accessory pulsatile organs (auxiliary hearts) in the mosquito *Anopheles gambiae*

Sushma Boppana and Julián F. Hillyer*

ABSTRACT

Mosquito antennae provide sensory input that modulates host-seeking, mating and oviposition behaviors. Thus, mosquitoes must ensure the efficient transport of molecules into and out of these appendages. To accomplish this, mosquitoes and other insects have evolved antennal accessory pulsatile organs (APOs) that drive hemolymph into the antennal space. This study characterizes the structural mechanics of hemolymph propulsion throughout the antennae of *Anopheles gambiae*. Using intravital video imaging, we show that mosquitoes possess paired antennal APOs that are located on each side of the head's dorsal midline. They are situated between the frons and the vertex in an area that is dorsal to the antenna but ventral to the medial-most region of the compound eyes. Antennal APOs contract in synchrony at 1 Hz, which is 45% slower than the heart. By means of histology and intravital imaging, we show that each antennal APO propels hemolymph into the antenna through an antennal vessel that traverses the length of the appendage and has an effective diameter of 1–2 μm. When hemolymph reaches the end of the appendage, it is discharged into the antennal hemocoel and returns to the head. Because a narrow vessel empties into a larger cavity, hemolymph travels up the antenna at 0.2 mm s⁻¹ but reduces its velocity by 75% as it returns to the head. Finally, treatment of mosquitoes with the anesthetic agent FlyNap (triethylamine) increases both antennal APO and heart contraction rates. In summary, this study presents a comprehensive functional characterization of circulatory physiology in the mosquito antennae.

KEY WORDS: Antenna, Hemocoel, Circulatory physiology, Antennal heart, Heart, Vessel

INTRODUCTION

The antennae of insects are involved in the detection of chemical, tactile, thermal and auditory stimuli (Chapman and Simpson, 2013). The antennae also mechanically assist during the mating of fleas, and contain the timing elements of the sun compass that drives the autumn migration of monarch butterflies (Hsu and Wu, 2001; Merlin et al., 2009). In mosquitoes, the detection of near-field sound by the antennae's Johnston's organs influences courtship and mating, and the reception of odorant and thermal cues by antennal receptor neurons controls oviposition and host-seeking behaviors (Cator et al., 2009; Wang et al., 2009; Carey et al., 2010; Rinker et al., 2013). Because antennae are intricately involved in essential physiological processes, insects must ensure that molecules required for proper

Department of Biological Sciences, Vanderbilt University, Nashville, TN 37235, USA.

*Author for correspondence (julian.hillyer@vanderbilt.edu)

antennal functioning are efficiently transported into and out of these peripheral sensory appendages.

The primary manner by which insects transport nutrients, hormones, waste and other molecules from one region of the body to another is by circulating a fluid medium called hemolymph through an open body cavity called the hemocoel (Chapman et al., 2013; Klowden, 2013). The main pump that drives hemolymph circulation is called the dorsal vessel, which is a muscular tube that extends from the insect's head to the posterior of the abdomen and is anatomically divided into a thoracic aorta and an abdominal heart (Jones, 1977; Wasserthal, 2007; Glenn et al., 2010; Wirkner et al., 2013). Although effective in circulating hemolymph across the central body cavity, this pump does not produce sufficient directional force to drive hemolymph to all regions of the organism. To overcome this limitation, insects have evolved a series of structurally independent accessory pulsatile organs (APOs or auxiliary hearts) that either propel or assist in the propulsion of hemolymph through narrow, dead-end appendages and through the ventral extracardiac space (Pass, 2000; Pass et al., 2006; Andereck et al., 2010). Specifically, these APOs drive hemolymph through the antennae, wings, head, ventral abdomen, and abdominal appendages such as the cerci (Wasserthal, 1980; Hertel et al., 1985; Hustert, 1999; Wasserthal, 1999; Gereben-Krenn and Pass, 2000; Pass, 2000; Sláma, 2008; Andereck et al., 2010).

In most insect orders, hemolymph flows into the antennae through the active contractility of antennal APOs, which are also known as antennal hearts (Pass, 2000; Pass et al., 2006; Wirkner et al., 2013). Antennal APOs show remarkable structural variability across taxa, but their general plan involves an ampulla located in the head that forces hemolymph into the antennae by means of an antennal vessel (Clements, 1956; Pass, 1980; Pass, 1985; Pass, 1991; Sun and Schmidt, 1997; Matus and Pass, 1999). Although the structure of antennal APOs has been thoroughly investigated in multiple insect orders, the functional mechanics of hemolymph flow through these appendages remain poorly understood. This is primarily because the circulation of hemolymph through the antennae has been inferred from structural analyses and not from active visualizations of flow. Nevertheless, several studies in Blattodea and other Polyneoptera (lower Neoptera) have described the contractile and neurohemal activity of antennal hearts, illustrating the physiological complexity of these APOs (Hertel et al., 1985; Pass et al., 1988; Lange et al., 1993; Richter and Hertel, 1997; Predel, 2001; Hertel et al., 2012).

The goal of the present study was to characterize the functional mechanics of antennal accessory pulsatile organs in the African malaria mosquito *Anopheles gambiae* Giles 1902 *sensu stricto* (Diptera: Culicidae: Anophelinae). The structure of antennal APOs has been described for the yellow fever mosquito, *Aedes aegypti* (Diptera: Culicidae: Culicinae), but physiological data on these

organs are lacking (Clements, 1956; Sun and Schmidt, 1997). Here, using novel fluorescence-based methods we (1) determined the contraction rate of anopheline antennal APOs, (2) show that the antennal APOs contract in a manner that is independent of the heart, (3) determined the effective diameter of the antennal vessel, (4) measured the directional velocity of hemolymph as it travels across the antennal space, (5) describe the structure of the antennal APOs and the antennal vessel, and (6) show that the anesthetic agent FlyNap (active ingredient: triethylamine) accelerates both heart and antennal APO contractions rates.

RESULTS

Antennal APOs are located between the frons and the vertex, and contract in synchrony

Contractions of the *A. gambiae* heart can be observed by illuminating the abdomen using trans-brightfield light (Glenn et al., 2010; Hillyer et al., 2012; Chen and Hillyer, 2013; Estévez-Lao et al., 2013). However, the small size of the antennal APOs, together with the lack of translucency of the head, does not allow for their visualization using brightfield illumination. In order to visualize the antennal APOs in live and intact mosquitoes, we developed a novel fluorescence-based method that relies on the action of the heart. Specifically, fluorescent microspheres that are injected into the hemocoel are disseminated to all parts of the body by the contractile action of the heart (Andereck et al., 2010; Glenn et al., 2010). Some of these microspheres aggregate in and around the antennal APOs, and the contraction of the APOs results in a spatial shift of these fluorescent aggregates (supplementary material Movie 1). Thus, by visualizing the oscillations of the fluorescent aggregates that form in and around each antennal APO, we were able to identify their location and monitor their contraction.
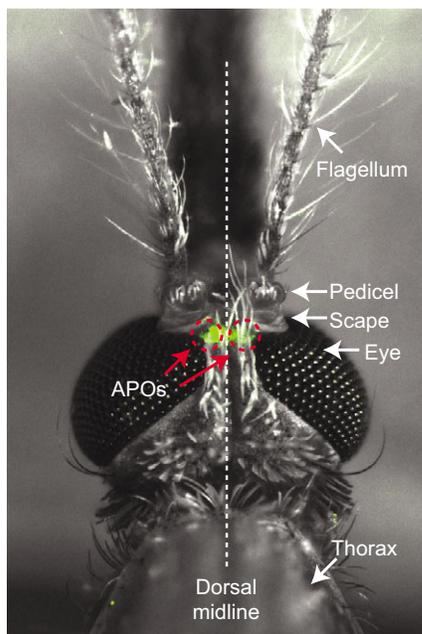

Fig. 1. Location of the antennal accessory pulsatile organs (APOs) in *Anopheles gambiae*. Brightfield and fluorescence overlay showing the antennal APOs (green fluorescence inside red circles). The APOs are located in the head between the frons and the vertex in an area that flanks the dorsal midline of the mosquito. The APOs are dorsal and posterior to the antenna's scape and pedicel, but ventral to the medial-most region of the compound eyes.

Anopheles gambiae possess two antennal APOs that are located on each side of the head's dorsal midline (Fig. 1). These APOs abut against the cuticle and are located between the frons and the vertex in an area that is dorsal and posterior to the base of the antenna but ventral to the medial-most region of the compound eyes. Intravital video imaging of the *A. gambiae* head revealed that the left and the right antennal APOs contract at an average rate of 0.976 and 0.974 Hz, respectively (Fig. 2A; paired *t*-test $P=0.8127$). There was a strong correlation between the contraction rates of the left and right antennal APOs (Fig. 2B; $R=0.974$; Pearson correlation $P<0.0001$), and 78% of the mosquitoes sampled had APOs that differed by ≤3 contractions min^{-1} (Fig. 2C; mean 59 contractions min^{-1}). Graphical analysis of APO contractions revealed that the APOs contract in synchrony, signifying that the two APOs are either linked or are controlled by the same mechanism (Fig. 3A,B). When one APO skips a beat, graphical analysis of the skip shows a minimal but observable change in the intensity profile of the APO, indicating that the skipped beat involves a weak contraction that is likely not effective in propelling hemolymph (Fig. 3C). In support of the observation that the two APOs contract in harmony, when an APO skips a beat, the two accessory hearts immediately return to contracting in sync. Likewise, in the instances where both APOs stop contracting (when this occurs, they usually stop for 2–3 s), the two APOs pause simultaneously and then return to their contracting state at the same time. Finally, although the heart reverses contraction direction approximately 10 times per minute (Hillyer et al., 2012; Estévez-Lao et al., 2013), antennal APO contractions are normally continuous over the course of each 60 s recording. That is, when videos are broken down into smaller intervals, the contraction rates remain the same, and the mechanics of individual contractions do not change during the course of each recording.

Antennal APOs and the heart are not synchronized

Immediately following the physiological recording of the antennal APOs, the heart of these same mosquitoes was also monitored (supplementary material Movie 2). In contrast to the antennal APOs, which on average contracted at 0.97 Hz, the heart contracted at 1.808 Hz (Fig. 2A; repeated measures ANOVA $P<0.0001$). There was no correlation between the contraction rates of the antennal APOs and the heart (Fig. 2D; $R=0.165$; Pearson correlation $P=0.196$), and graphical analyses of individual contractions failed to detect any kind of correlation between heart and antennal APO contractions (Fig. 3A,B,D,E).

Hemolymph velocity changes as it travels across the antennal space

Qualitative observations of the movement of 1 μm diameter fluorescent microspheres that had been injected into the hemocoel revealed that they enter the antennal APOs and are propelled into the antennal space. These 1 μm microspheres travel in a linear trajectory up the antenna (away from the head) along the lateral portion of the appendage that is closest to the dorsal midline of the mosquito. Upon reaching the distal end of the antenna, the microspheres turn medially and begin a downward trajectory (toward the head) along the medial and lateral portions of the antenna (supplementary material Movie 3). This downward movement, while linear, displays more lateral mobility and is slower than when microspheres travel in the upward direction.

When differently sized microspheres were injected into the hemocoel, we observed that 2 μm diameter microspheres rarely aggregated in or around the antennal APOs, and these microspheres
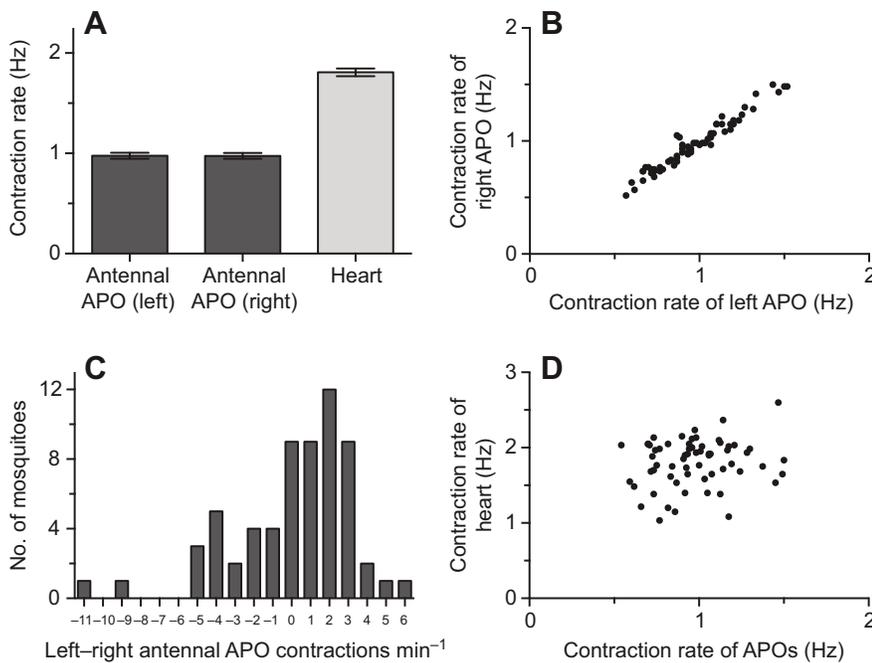
Fig. 2. Antennal APO and heart contraction rates.
(A) Contraction rates of the left and right antennal APOs and the heart. Sample size is 63 and whiskers denote the s.e.m. (B) Correlation between the contraction rates of the left and right antennal APOs of each mosquito (R=0.974). (C) Difference in the number of contractions per minute between the left and right antennal APOs of each mosquito. (D) Correlation between the contraction rates of the antennal APOs (average of left and right) and the heart of each mosquito (R=0.165). All mosquitoes were anesthetized by brief exposure to cold temperature.

did not enter the antennal space. In contrast, 1 and 0.5 μm diameter microspheres were always observed in and around the antennal APOs and in the antennal space. However, while the flow of 0.5 μm diameter microspheres was efficient and unimpeded, the flow of 1 μm diameter microspheres met some degree of resistance; 1 μm diameter microspheres at times stopped moving, indicating that they became stuck within antennal structures. These data suggest that the effective circulatory diameter of the mosquito antenna is between 1 and 2 μm in diameter.

Given that 0.5 μm diameter microspheres flow freely across the antennal space, the movement of these neutrally buoyant particles was tracked to quantitatively measure hemolymph flow within this appendage (Fig. 4). Microspheres were tracked for nearly identical distances when moving in the upward and downward directions (mean ± s.d., 683±125 and 687±134 μm, respectively; t-test P=0.8835), and, on average, microspheres moved up the antenna at a velocity of 197.0 μm s^{-1} and down the antenna at 51.7 μm s^{-1} (t-test P<0.0001). Furthermore, the maximum acceleration of microspheres averaged 13,797 μm s^{-2} when moving up the antenna but only 3067 μm s^{-2} when traveling down the antenna (t-test P<0.0001). This reduction in velocity and maximum acceleration as hemolymph transitions from moving upward to moving downward supports the antennal vessel hypothesis of hemolymph movement across the antennal space.

Structure of the antennal APOs and the antennal vessel
To confirm the hypothesis that hemolymph enters the antennae through an antennal vessel and returns to the head through a wider antennal hemocoel, mosquito heads were embedded, sectioned and visualized by brightfield microscopy. Earlier work in *A. aegypti* has extensively described the structural organization of antennal APOs in culicine mosquitoes (Clements, 1956; Sun and Schmidt, 1997). Here, by means of a comparative anatomy approach that relied on the descriptions by Sun and Schmidt as a point of reference (Sun and Schmidt, 1997), we identified in *A. gambiae* many of the same structures described in *A. aegypti*. Mainly, each APO contains a chamber, or ampulla, that includes a septum-like structure that has

been hypothesized to function as a valve (Fig. 5A) (Sun and Schmidt, 1997). The posterior of the chamber is attached to the z-body whereas the anterior is attached to cuticular epidermis (Fig. 5A). The z-body is composed of dense groups of cells, and is attached to muscle that drives antennal APO contractions. Specifically, muscle contraction expands (dilates) the ampulla, filling it with hemolymph. Then, muscle relaxation returns the ampulla to a more compact shape, forcing hemolymph into the antenna. Thus, mosquito antennal APOs are of the ampulla dilator type (Sun and Schmidt, 1997; Pass, 2000; Pass et al., 2006), and they propel hemolymph via passive systole. Interestingly, we observed that the anterior of the ampulla attaches to cells that do not resemble the columnar cells previously described in culicines. However, it is possible, and even likely, that the angle of sectioning employed in this study could not properly capture the shape or structure of these cells.

Hemolymph that enters the ampulla of an APO is driven into the antenna by means of an antennal vessel (Fig. 5B–E). The antennal vessel exits the APO, crosses the Johnston's organ located in the pedicel, enters the flagellum, and extends along the lateral portion of the antenna that is closest to the dorsal midline of the mosquito. The antennal vessel ends near the distal portion of the flagellum, where hemolymph is discharged into the antennal cavity and returns to the hemocoel via the medial and lateral portions of the antennal hemocoel (Fig. 5F).

FlyNap increases antennal APO and heart contraction rates
We have previously reported that exposing mosquitoes to FlyNap increases heart contraction rates and eliminates the cardio-acceleratory effect of the neuropeptide CCAP (Chen and Hillyer, 2013). To test whether exposing mosquitoes to FlyNap induces a similar effect on the antennal APOs, we anesthetized groups of mosquitoes with either cold or FlyNap and measured both antennal APO and heart contraction rates.

Observations of the dorsal abdomen revealed that the heart of mosquitoes exposed to FlyNap contracts 15% faster than the heart of mosquitoes anesthetized by exposure to cold temperatures
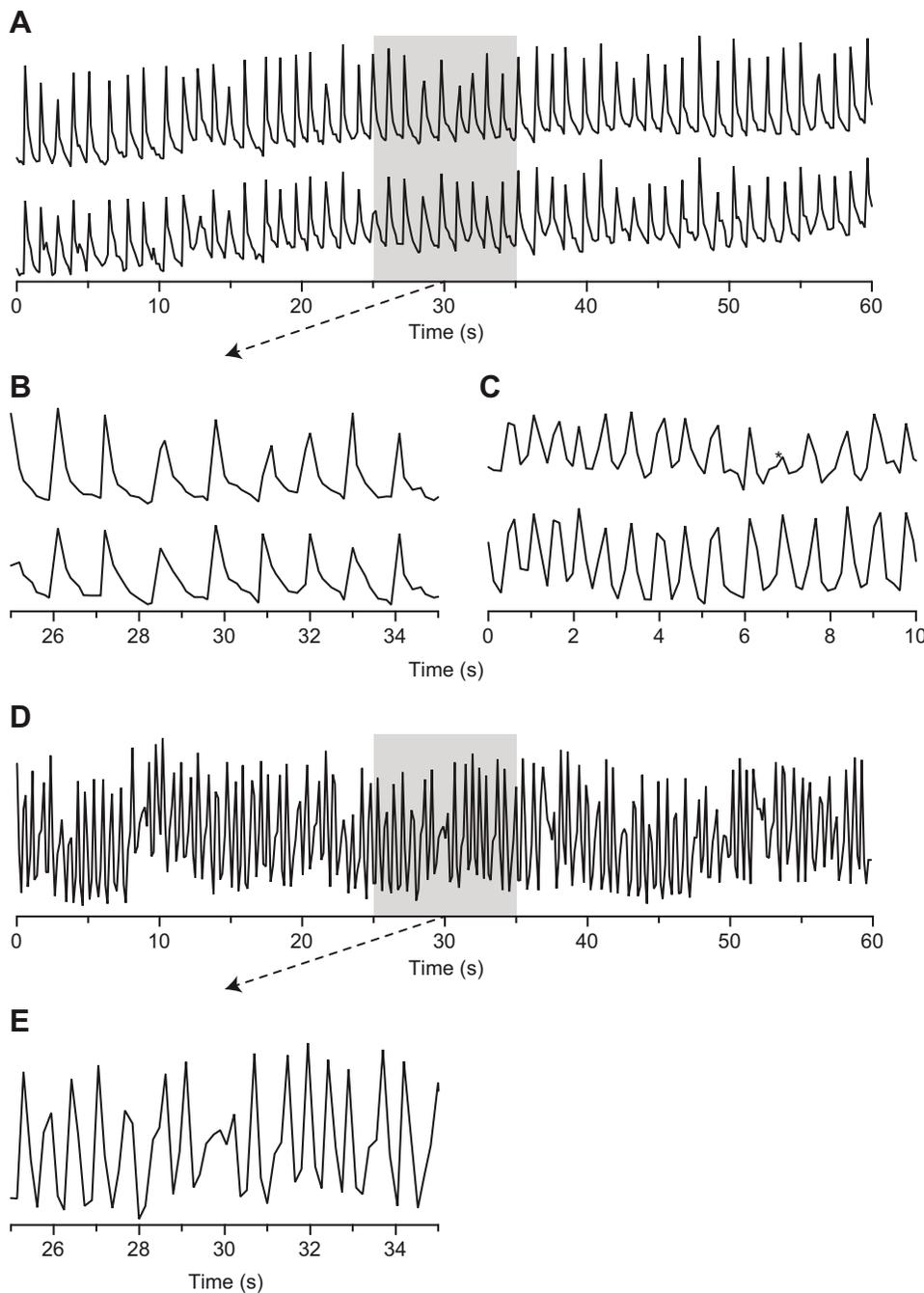
Fig. 3. Graphical representation of antennal APO and heart contractions. (A,B) Graphical representation of the contractions of the left (top) and right (bottom) APOs of a mosquito. Each peak represents a contraction and the area shaded in A is magnified in B. (C) Graphical representation of left (top) and right (bottom) APO contractions in a different mosquito, showing a skipped beat (asterisk). Comparison of B and C illustrates the natural variability of antennal APO contraction rates. (D,E) Graphical representation of heart contractions in the mosquito shown in A. Each peak represents a contraction and the area shaded in D is magnified in E. Videos used to create A and D show the same mosquito but were acquired approximately 1 min apart. All mosquitoes were anesthetized by brief exposure to cold temperature.

(Fig. 6A; t-test P=0.0018), which is in line with our earlier observations (Chen and Hillyer, 2013). Observations of the head revealed that the left and right antennal APOs of mosquitoes exposed to FlyNap contract 29% faster (both APOs) than the APOs of mosquitoes exposed to cold (Fig. 6A; t-test P=0.0001 and P<0.0001 for the left and right APOs, respectively). When the entire dataset was analyzed by two-way repeated measures ANOVA, the heart was found to contract faster than the APOs (P<0.0001), and pumping organs (heart and APOs) exposed to FlyNap contracted faster than pumping organs exposed to cold (P<0.0001). However, there was no interaction between the anesthetic agent and the pumping organ, indicating that exposure to FlyNap did not induce different effects on the heart and the antennal APOs (P=0.9988).

There was a strong correlation between the contraction rates of the left and right antennal APOs following both cold (R=0.966; Pearson correlation P<0.0001) and FlyNap (R=0.901; Pearson correlation P<0.0001) anesthesia, but there was no correlation between antennal APO and heart contraction rates following exposure to either anesthetic agent (cold R=0.092 and Pearson correlation P=0.683; FlyNap R=0.092 and Pearson correlation P=0.683; Fig. 6B,D). However, a higher proportion of mosquitoes exposed to FlyNap had APOs that did not contract in perfect synchrony, and these APOs also exhibited higher variability in the difference in contractions per minute between antennal APOs. Specifically, whereas 77% of the mosquitoes exposed to cold anesthesia had APOs that differed by ≤3 contractions min⁻¹, this value was only 68% for mosquitoes exposed to FlyNap (Fig. 6C). Perhaps this difference is due to the fact
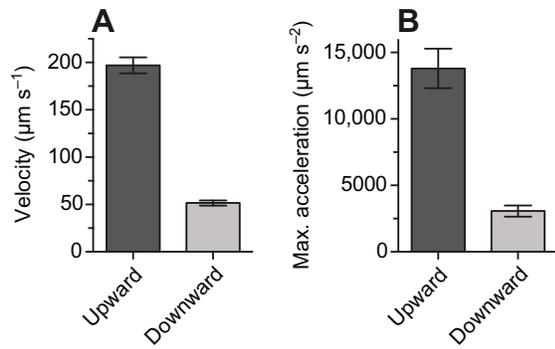
Fig. 4. Velocity and maximum acceleration of hemolymph as it travels across the antennal space. Velocity (A) and maximum acceleration (B) of 0.5 µm diameter microspheres as they travel upward (away from the head) and downward (returning to the head) within the antennal space. Sample size is 63 in each direction and whiskers denote the s.e.m. All mosquitoes were anesthetized by brief exposure to cold temperature.

that mosquitoes exposed to FlyNap have higher antennal APO contraction rates (mean 75 contractions min⁻¹ for FlyNap versus 58 contractions min⁻¹ for cold).

DISCUSSION

Antennal circulatory organs have been identified in numerous insect orders (Pass, 2000; Pass et al., 2006; Hertel et al., 2012). Common

amongst antennal circulatory organs is their function as a conduit that leads hemolymph into the antenna. However, antennal circulatory organs display remarkable structural variability across taxa. Nine different types have been structurally described, and these can be grouped into non-pulsatile organs, pulsatile organs where muscle contraction compresses the ampulla, and pulsatile organs where muscle contraction dilates the ampulla (Pass, 2000; Pass et al., 2006). Structural analyses in the culicine mosquito *A. aegypti* classified their antennal circulatory organs as members of the ampulla dilator type (Clements, 1956; Sun and Schmidt, 1997). In the present study, we used a correlative structural and functional approach to confirm that the mosquito antennal APOs are of the ampulla dilator type and describe for the first time the real-time functional mechanics of hemolymph propulsion across the antennal space.

Earlier structural analyses on the antennal APOs of *A. aegypti* described an ampulla that is attached to a z-body (also referred to as a syncytial body), which is attached to muscle that extends to the aorta (Clements, 1956; Sun and Schmidt, 1997). Contraction of this muscle expands the ampulla, forcing hemolymph from the head into the APO. When the muscle relaxes, the ampulla returns to a more compact size, driving hemolymph into the antenna by means of an antennal vessel. The structural and functional data presented herein are in agreement with this 'passive systole' model of hemolymph propulsion across the antennal space. First, histological experiments showed that the structural organization of *A. gambiae* and *A. aegypti* antennal APOs is similar. Second,
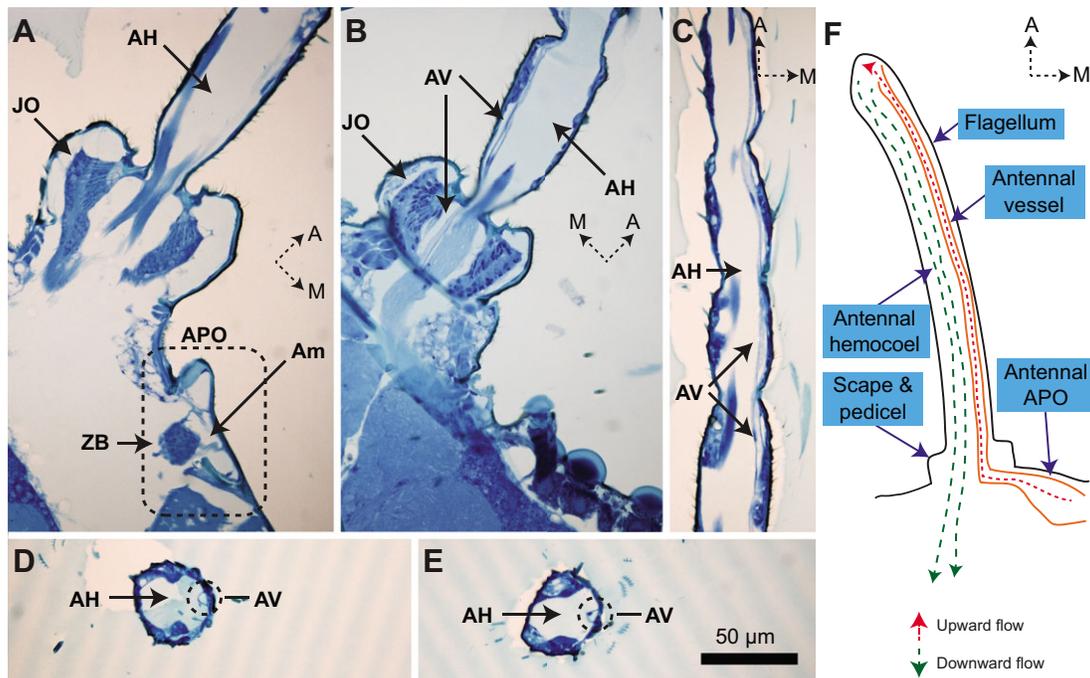

Fig. 5. Structure of the antennal APOs and the antennal vessel. (A) Histological section of the head and antenna showing an antennal APO that contains an ampulla (Am; chamber) that is attached anteriorly to the cuticular epidermis and posteriorly to the z-body (ZB). An antennal vessel (AV) extends from the APO and travels up the scape and pedicel containing the Johnston's organ (JO) and through the antennal hemocoel (AH). (B) Histological section of the head and antenna showing the antennal vessel extending across the Johnston's organ and through the antennal hemocoel. (C) Coronal section of an antenna showing the antennal vessel and the antennal hemocoel. (D,E) Cross-section of two different antennae showing the antennal vessel and the antennal hemocoel. (F) Model of hemolymph flow across the antennal space, based on flow data and histological data (structures are not drawn to scale). An antennal APO located in the head propels hemolymph into the antenna by means of an antennal vessel. When hemolymph reaches the distal end of the appendage it is released into a wider antennal hemocoel, or cavity, and it flows back toward the head. Because of the difference between the diameters of the antennal vessel and the antennal hemocoel, hemolymph velocity is four times higher in the upward direction than it is in the downward direction. A, anterior; M, medial (toward the dorsal midline of the mosquito). Scale bar applies to all micrographs.
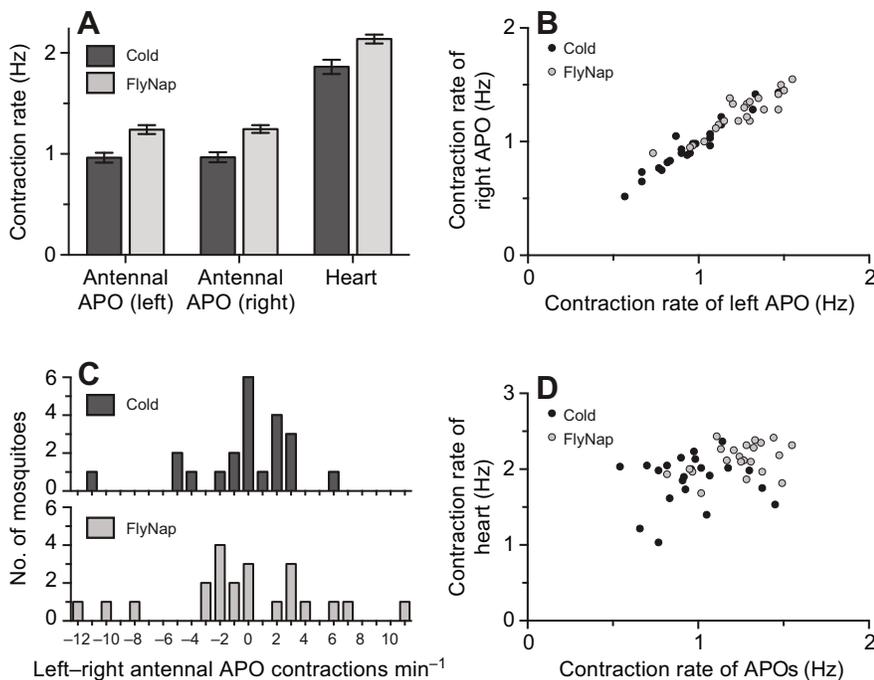
Fig. 6. Antennal APO and heart contraction rates following cold or FlyNap (triethylamine) anesthesia. (A) Contraction rates of the left and right antennal APOs and the heart following cold or FlyNap anesthesia. For each anesthetic agent, sample size is 22 and whiskers denote the s.e.m. (B) Correlation between the contraction rates of the left and right antennal APOs of each mosquito following cold (R=0.966) or FlyNap (R=0.901) anesthesia. (C) Difference in contractions per minute between the left and right antennal APOs of each mosquito following cold or FlyNap anesthesia. (D) Correlation between the contraction rates of the antennal APOs (average of left and right) and the heart of each mosquito following cold (R=0.092) or FlyNap (R=0.361) anesthesia.

intravital video imaging of the head showed that each APO contraction is manifested by a spatial shift toward the aorta that expands the ampulla and inflates it with hemolymph (dilatory movement; diastole), which is followed by a spatial shift that returns the APO to its original position, contracting the ampulla and driving hemolymph into the antenna (compressive movement; systole). Lastly, intravital video imaging of the antenna showed that hemolymph enters the appendage through a narrow antennal vessel and returns to the head via a wider antennal hemocoel. However, our model of hemolymph flow across the antennal space differs from earlier descriptions of mosquito antennal APOs in one key respect. Based on their structural observations, Sun and Schmidt (Sun and Schmidt, 1997) proposed that dilation of the ampulla, besides driving hemolymph from the head into the APO, also results in backflow from the antennal vessel. Our functional visualizations of flow showed no evidence of backflow: flow through the antennal vessel is unidirectional.

Mosquito antennal APOs contract at ~1 Hz whereas the heart contracts at ~1.8 Hz. Contractions of antennal APOs, while synchronized with one another, are not synchronized with the heart. Comparison of these findings with earlier reports is difficult, as few studies have reported absolute antennal APO contraction rates, and these studies have largely focused on Polyneoptera (Hertel et al., 1985; Lange et al., 1993; Hertel et al., 2012), a group of insects that is distantly related to mosquitoes (Trautwein et al., 2012). Nevertheless, one of these studies showed that the antennal APOs and the heart of the American cockroach, *Periplaneta americana*, are not synchronized, and that the 0.45 Hz antennal APO contraction rate is significantly slower than the 1.28 Hz contraction rate of the dorsal vessel (Hertel et al., 2012).

To date, the path of hemolymph flow across the insect antennae has been inferred from a combination of structural analyses and the visualization of APO contractions. Unique to the present work is the direct visualization and measurement of hemolymph flow velocity across the antennal space. Specifically, by adapting methodologies we have previously used to measure the directional velocity of hemolymph inside the heart and in other regions of the abdomen

(Andereck et al., 2010; Glenn et al., 2010; Estévez-Lao et al., 2013), we showed that hemolymph typically travels up the mosquito antennae at 197 μm s^{-1} and down the antenna at 52 μm s^{-1}. Hemolymph velocity through the antenna is one to two orders of magnitude slower than hemolymph flow through the heart (Glenn et al., 2010; Estévez-Lao et al., 2013). Furthermore, antennal hemolymph velocity in the upward direction is comparable to flow velocity in the extracardiac abdomen, but antennal flow velocity in the downward direction is ~75% slower than flow velocity in the abdominal cavity (Andereck et al., 2010).

In addition to providing direct information on flow, these hemolymph flow data provide functional evidence supporting our model of hemolymph propulsion across the antennal space. Specifically, the finding that microspheres reduce their velocity and maximum acceleration by 74% and 54%, respectively, as they shift from going upward to going downward, together with the observation that microspheres move in a linear manner when traveling up the antenna but experience slight lateral movements when traveling down the antenna, supports the antennal vessel model of hemolymph propulsion. That is, microspheres moving up a narrow antennal vessel are predicted to travel faster and straighter than particles returning through a wider cavity. Similarly, maximum acceleration is predicted to decrease as microspheres move away from the contractile pump. This model also explains why hemocytes are seldom, if ever, observed inside the antennae (King and Hillyer, 2013): tracking of differently sized microspheres showed that the effective diameter of the antennal vessel is 1–2 μm, which is significantly smaller than the ~10 μm diameter of circulating hemocytes.

Finally, we recently showed that exposing mosquitoes to FlyNap (triethylamine) increases heart contraction rates and eliminates the cardioacceleratory effect of the neurohormone CCAP (Chen and Hillyer, 2013). FlyNap is commonly used in studies assessing heart activity in *Drosophila melanogaster* (Paternostro et al., 2001; Wessells and Bodmer, 2004; Lo et al., 2007; Neckameyer and Matsuo, 2008; Choma et al., 2010; Tsai et al., 2011; Tang et al., 2014), and two of these studies detected differences in cardiac

function when the effect of FlyNap-based anesthesia was compared with other methods of insect restraint (Paternostro et al., 2001; Tsai et al., 2011). Our finding that exposure to FlyNap increases both antennal APO and heart contraction rates further cautions that FlyNap should be avoided in studies assessing circulatory physiology. Moreover, our FlyNap-based findings also support the hypothesis that the antennal APOs and the heart, while myogenic (Hertel et al., 1985; Richter and Hertel, 1997; Chapman et al., 2013; Klowden, 2013), are modulated by similar neural or hormonal stimuli. This hypothesis is also supported by two additional lines of evidence. First, antennal APOs have neurohemal function and are capable of producing myotropic factors (Pass et al., 1988; Predel, 2001). Second, in some insects the neuropeptide proctolin modulates antennal APO (Hertel et al., 1985; Lange et al., 1993; Hertel et al., 2012) and heart (Zornik et al., 1999; Sliwowska et al., 2001; Ejaz and Lange, 2008) contraction rates. Although proctolin is not produced by either *A. gambiae* or *A. aegypti* (Riehle et al., 2002; Predel et al., 2010), other cardiomyotropic peptides, such as CCAP and FMRFamide-related peptides, are produced by most arthropods, including mosquitoes (Orchard et al., 2001; Dulcis et al., 2005; Ejaz and Lange, 2008; Walker et al., 2009; Estévez-Lao et al., 2013; Hillyer et al., 2014).

There is little doubt that the insect circulatory system is among the most understudied of insect physiological systems (Harrison et al., 2012). The present study provides comprehensive answers to fundamental entomological questions and expands our understanding of the biology of hemolymph propulsion across sensory appendages. Moreover, this study also focused on an insect that is a significant pest and disease vector (Becker et al., 2010). Given that hemolymph currents influence the biology of pathogens in the hemocoel (King and Hillyer, 2012), and that mosquito antennae provide sensory input that drives processes involved in mating and host-seeking behaviors (Cator et al., 2009; Wang et al., 2009; Carey et al., 2010; Rinker et al., 2013), the data presented herein may also begin to shed new light on mosquito processes required for pathogen transmission, reproduction and blood feeding.

MATERIALS AND METHODS
Mosquito rearing and maintenance
Anopheles gambiae (G3 strain) were reared as described elsewhere (Estévez-Lao et al., 2013). Briefly, eggs were hatched in water, larvae were fed a mixture of koi food and yeast, and upon emergence adults were fed a 10% sucrose solution *ad libitum*. Mosquito rearing and maintenance were performed at 27°C and 75% relative humidity, under a 12 h light:12 h dark photoperiod. All experiments were performed on adult females at 4 or 5 days post-eclosion.

Mosquito anesthesia
Mosquitoes were anesthetized using cold-based or FlyNap-based anesthesia as described elsewhere (Chen and Hillyer, 2013). For cold-based anesthesia, mosquitoes were exposed to −20°C for 60 s, and were then transferred to a Petri dish that was placed over ice until use. For FlyNap-based anesthesia, mosquitoes were placed in a covered 60 cm³ enclosure and an absorbent wand that had been loaded with FlyNap (Carolina Biological Supply, Burlington, NC, USA) was introduced into the vessel for 30 s. Following exposure to FlyNap, mosquitoes were transferred to a Petri dish held at room temperature until use. Cold anesthesia knocks down mosquitoes for several minutes whereas FlyNap anesthesia (active ingredient: triethylamine) knocks down mosquitoes for several hours (Chen and Hillyer, 2013). The default anesthetic agent used in this study was cold, and only experiments explicitly labeled 'FlyNap' employed this form of chemical anesthesia.

Intravital video imaging of antennal accessory pulsatile organs and the heart
Each mosquito was anesthetized, visualized using a SMZ645 stereomicroscope (Nikon, Tokyo, Japan) and intrathoracically injected with ~0.1 μl of 0.2% solids 1 μm diameter yellow–green fluorescent (505/515) carboxylate-modified microspheres (Molecular Probes, Eugene, OR, USA) in PBS (pH 7.0). The legs and wings were severed with a razor blade, and the mosquito was placed dorsal side up between two rolled strips of Parafilm M (Pechiney Plastic Packaging Company, Chicago, IL, USA) on a glass slide. The mosquito head was rested on top of a flat piece of Parafilm and the slide was transferred to a Nikon 90i compound microscope equipped with a Nikon Intensilight C-HGFI fluorescence illumination unit, a Photometrics CoolSNAP HQ2 camera (Roper Scientific, Ottobrunn, Germany) and Nikon Advanced Research NIS Elements software. At 3–7 min post-injection, the mosquito was illuminated with low-level fluorescence (using a neutral density filter of 4), and a 60 s intravital video of the head, focusing on both antennal APOs, was acquired. Then, the heart was imaged through the dorsal abdomen, and another 60 s intravital video was acquired. This protocol yielded paired data, where each mosquito was imaged twice: once for the antennal APOs and once for the heart. The following video acquisition parameters were used: 3×3 binning, 4× gain and 10 ms exposure with no delay.

The contraction of antennal APOs was measured by visualizing the movement of fluorescent aggregates in the anterior–dorsal portion of the head. Absolute contraction rates were determined by manually counting the oscillation of the fluorescent aggregates associated with each APO. Graphical representations of individual antennal APO contractions were rendered using NIS Elements by selecting the area immediately surrounding each antennal APO and then quantifying how the sum light intensity changed as each contraction shifted the fluorescent aggregate out of and into the selected area. For visualization ease, all values were multiplied by −1 such that each peak (not valley) marks a contraction.

Heart contractions were measured by counting the wave-like contractions of the abdominal heart (Glenn et al., 2010). Graphical representations of heart contractions were rendered by monitoring the spatial fluorescence oscillations of periostial hemocytes that had phagocytosed fluorescent microspheres on the surface of the heart (King and Hillyer, 2012). As for the antennal APOs, all values were multiplied by −1 such that each peak marks a contraction. Finally, although the mosquito heart periodically alternates between contracting in anterograde (toward the head) and retrograde (toward the posterior abdomen) directions, in this study we only measured the total heart rate as heart rhythmicity in mosquitoes does not change with contraction direction (Andereck et al., 2010; Glenn et al., 2010; Hillyer et al., 2012; Chen and Hillyer, 2013; Estévez-Lao et al., 2013), and antennal APO contractions were evenly distributed across time. For cold anesthesia, 63 mosquitoes were included in the analysis. For the experiment testing the difference between cold anesthesia and FlyNap anesthesia, 22 mosquitoes were analyzed per treatment.

Measurement of hemolymph flow distance, velocity and acceleration
To track hemolymph flow within the antenna, mosquitoes were cold anesthetized and injected with ~0.1 μl of 0.02% solids 0.5 μm diameter yellow–green fluorescent (505/515) carboxylate-modified microspheres in PBS. Mosquitoes were positioned on a slide ventral side up with both antennae lying flat on a strip of Parafilm, and the legs and wings held down by two additional strips of Parafilm. One antenna per mosquito was imaged using the same set-up and acquisition parameters used to monitor APO contractions, and a 60 s low-level fluorescence video was recorded. The manual feature of the Object Tracker module of NIS-Elements was used to quantitatively track the trajectory of neutral density microspheres as they flowed up or down the antennae. Then, the distance traveled, velocity and maximum acceleration of each microsphere were calculated (Andereck et al., 2010; Glenn et al., 2010). A total of 21 mosquitoes were assayed, and for each mosquito, three microspheres were tracked while moving up the antenna (away from the head) and three microspheres were tracked while they moved down the antenna (toward the head).

Histology

Mosquitoes were decapitated, and their heads were fixed by immersion in 4% formaldehyde in $0.1\,\mathrm{mol\,l^{-1}}$ phosphate buffer (pH 7.0) for 2 h. Specimens were dehydrated through a graded ethanol series, infiltrated with JB4-Plus resin (Electron Microscopy Sciences, Hatfield, PA, USA), and embedded in polyethylene molding trays anaerobically sealed with block holders and wax. Serial sections of 2.5 μm thickness were cut using a glass knife on a Sorvall JB-4 microtome (Sorvall, Newtown, CT, USA), placed on glass slides, and stained with Azure II. The slides were dried, coverslips were mounted using Poly-Mount (Polysciences Inc., Warrington, PA, USA), and the sections were imaged using the 90i microscope connected to a Nikon DS-Fi1 high-definition color CCD camera (Glenn et al., 2010).

References

Andereck, J. W., King, J. G. and Hillyer, J. F. (2010). Contraction of the ventral abdomen potentiates extracardiac retrograde hemolymph propulsion in the mosquito hemocoel. *PLoS ONE* **5**, e12943.

Becker, N., Petric, D., Zgomba, M., Boase, C., Dahl, C., Madon, M. and Kaiser, A. (2010). *Mosquitoes and Their Control*. New York, NY: Springer-Verlag.

Carey, A. F., Wang, G., Su, C. Y., Zwiebel, L. J. and Carlson, J. R. (2010). Odorant reception in the malaria mosquito *Anopheles gambiae*. *Nature* **464**, 66-71.

Cator, L. J., Arthur, B. J., Harrington, L. C. and Hoy, R. R. (2009). Harmonic convergence in the love songs of the dengue vector mosquito. *Science* **323**, 1077-1079.

Chapman, R. F. and Simpson, S. J. (2013). Head. In *The Insects: Structure and Function* (ed. S. J. Simpson and A. E. Douglas), pp. 3-14. Cambridge: Cambridge University Press.

Chapman, R. F., Douglas, A. E. and Siva-Jothy, M. T. (2013). Circulatory system, blood and the immune system. In *The Insects: Structure and Function* (ed. S. J. Simpson and A. E. Douglas), pp. 107-131. Cambridge: Cambridge University Press.

Chen, W. and Hillyer, J. F. (2013). FlyNap (triethylamine) increases the heart rate of mosquitoes and eliminates the cardioacceleratory effect of the neuropeptide CCAP. *PLoS ONE* **8**, e70414.

Choma, M. A., Suter, M. J., Vakoc, B. J., Bouma, B. E. and Tearney, G. J. (2010). Heart wall velocimetry and exogenous contrast-based cardiac flow imaging in *Drosophila melanogaster* using Doppler optical coherence tomography. *J. Biomed. Opt.* **15**, 056020.

Clements, A. N. (1956). The antennal pulsating organs of mosquitoes and other Diptera. *Q. J. Microsc. Sci.* **97**, 429-433.

Dulcis, D., Levine, R. B. and Ewer, J. (2005). Role of the neuropeptide CCAP in *Drosophila* cardiac function. *J. Neurobiol.* **64**, 259-274.

Ejaz, A. and Lange, A. B. (2008). Peptidergic control of the heart of the stick insect, *Baculum extradentatum*. *Peptides* **29**, 214-225.

Estévez-Lao, T. Y., Boyce, D. S., Honegger, H. W. and Hillyer, J. F. (2013). Cardioacceleratory function of the neurohormone CCAP in the mosquito *Anopheles gambiae*. *J. Exp. Biol.* **216**, 601-613.

Gereben-Krenn, B. A. and Pass, G. (2000). Circulatory organs of abdominal appendages in primitive insects (Hexapoda: Archaeognatha, Zygentoma and Ephemeroptera). *Acta Zool.* **81**, 285-292.

Glenn, J. D., King, J. G. and Hillyer, J. F. (2010). Structural mechanics of the mosquito heart and its function in bidirectional hemolymph transport. *J. Exp. Biol.* **213**, 541-550.

Harrison, J. F., Woods, H. A. and Roberts, S. P. (2012). *Ecological and Environmental Physiology of Insects*. New York, NY: Oxford University Press.

Hertel, W., Pass, G. and Penzlin, H. (1985). Electrophysiological investigation of the antennal heart of *Periplaneta americana* and its reactions to proctolin. *J. Insect Physiol.* **31**, 563-572.

Hertel, W., Neupert, S. and Eckert, M. (2012). Proctolin in the antennal circulatory system of lower Neoptera: a comparative pharmacological and immunohistochemical study. *Physiol. Entomol.* **37**, 160-170.

Hillyer, J. F., Estévez-Lao, T. Y., Funkhouser, L. J. and Aluoch, V. A. (2012). *Anopheles gambiae corazonin*: gene structure, expression and effect on mosquito heart physiology. *Insect Mol. Biol.* **21**, 343-355.

Hillyer, J. F., Estévez-Lao, T. Y. and de la Parte, L. E. (2014). Myotropic effects of FMRFamide containing peptides on the heart of the mosquito *Anopheles gambiae*. *Gen. Comp. Endocrinol.* **202**, 15-25.

Hsu, M. H. and Wu, W. J. (2001). Off-host observations of mating and postmating behaviors in the cat flea (Siphonaptera: Pulicidae). *J. Med. Entomol.* **38**, 352-360.

Hustert, R. (1999). Accessory hemolymph pump in the mesothoracic legs of locusts, (*Schistocerca gregaria* Forskal) (Orthoptera, Acrididae). *Int. J. Insect Morphol.* **28**, 91-96.

Jones, J. C. (1977). *The Circulatory System of Insects*. Springfield, IL: Charles C. Thomas.

King, J. G. and Hillyer, J. F. (2012). Infection-induced interaction between the mosquito circulatory and immune systems. *PLoS Pathog.* **8**, e1003058.

King, J. G. and Hillyer, J. F. (2013). Spatial and temporal in vivo analysis of circulating and sessile immune cells in mosquitoes: hemocyte mitosis following infection. *BMC Biol.* **11**, 55.

Klowden, A. J. (2013). Circulatory systems. In *Physiological Systems in Insects*, pp. 365-413. Boston, MA: Academic Press.

Lange, A. B., Chan, K. K. and Stay, B. (1993). Effect of allatostatin and proctolin on antennal pulsatile organ and hindgut muscle in the cockroach, *Diploptera punctata*. *Arch. Insect Biochem. Physiol.* **24**, 79-92.

Lo, P. C., Zaffran, S., Sénatore, S. and Frasch, M. (2007). The *Drosophila* Hand gene is required for remodeling of the developing adult heart and midgut during metamorphosis. *Dev. Biol.* **311**, 287-296.

Matus, S. and Pass, G. (1999). Antennal circulatory organ of *Apis mellifera* L. (Hymenoptera: Apidae) and other Hymenoptera: functional morphology and phylogenetic aspects. *Int. J. Insect Morphol.* **28**, 97-109.

Merlin, C., Gegear, R. J. and Reppert, S. M. (2009). Antennal circadian clocks coordinate sun compass orientation in migratory monarch butterflies. *Science* **325**, 1700-1704.

Neckameyer, W. S. and Matsuo, H. (2008). Distinct neural circuits reflect sex, sexual maturity, and reproductive status in response to stress in *Drosophila melanogaster*. *Neuroscience* **156**, 841-856.

Orchard, I., Lange, A. B. and Bendena, W. G. (2001). FMRFamide-related peptides: a multifunctional family of structurally related neuropeptides in insects. *Adv. Insect Physiol.* **28**, 267-329.

Pass, G. (1980). The anatomy and ultrastructure of the antennal circulatory organs in the cockchafer beetle *Melolontha melolontha* L. (Coleoptera, Scarabaeidae). *Zoomorphology* **96**, 77-89.

Pass, G. (1985). Gross and fine structure of the antennal circulatory organ in cockroaches (Blattodea, Insecta). *J. Morphol.* **185**, 255-268.

Pass, G. (1991). Antennal circulatory organs in Onychophora, Myriapoda and Hexapoda: functional morphology and evolutionary implications. *Zoomorphology* **110**, 145-164.

Pass, G. (2000). Accessory pulsatile organs: evolutionary innovations in insects. *Annu. Rev. Entomol.* **45**, 495-518.

Pass, G., Sperk, G., Agricola, H., Baumann, E. and Penzlin, H. (1988). Octopamine in a neurohemal area within the antennal heart of the American cockroach. *J. Exp. Biol.* **135**, 495-498.

Pass, G., Gereben-Krenn, B. A., Merl, M. and Plant, J. (2006). Phylogenetic relationships of the orders in Hexapoda: contributions from the circulatory organs for a morphological data matrix. *Arthropod Syst. Phylogeny* **64**, 165-203.

Paternostro, G., Vignola, C., Bartsch, D. U., Omens, J. H., McCulloch, A. D. and Reed, J. C. (2001). Age-associated cardiac dysfunction in *Drosophila melanogaster*. *Circ. Res.* **88**, 1053-1058.

Predel, R. (2001). Peptidergic neurohemal system of an insect: mass spectrometric morphology. *J. Comp. Neurol.* **436**, 363-375.

Predel, R., Neupert, S., Garczynski, S. F., Crim, J. W., Brown, M. R., Russell, W. K., Kahnt, J., Russell, D. H. and Nachman, R. J. (2010). Neuropeptidomics of the mosquito *Aedes aegypti*. *J. Proteome Res.* **9**, 2006-2015.

Riehle, M. A., Garczynski, S. F., Crim, J. W., Hill, C. A. and Brown, M. R. (2002). Neuropeptides and peptide hormones in *Anopheles gambiae*. *Science* **298**, 172-175.

Richter, M. and Hertel, W. (1997). Contributions to physiology of the antenna-heart in *Periplaneta americana* (L.) (Blattodea: Blattidae). *J. Insect Physiol.* **43**, 1015-1021.

Rinker, D. C., Pitts, R. J., Zhou, X., Suh, E., Rokas, A. and Zwiebel, L. J. (2013). Blood meal-induced changes to antennal transcriptome profiles reveal shifts in odor sensitivities in *Anopheles gambiae*. *Proc. Natl. Acad. Sci. USA* **110**, 8260-8265.

Sláma, K. (2008). Extracardiac haemocoelic pulsations and the autonomic neuroendocrine system (coelopulse) of terrestrial insects. *Terrestrial Arthropod Reviews* **1**, 39-80.

Sliwowska, J., Rosinski, G. and Nässel, D. R. (2001). Cardioacceleratory action of tachykinin-related neuropeptides and proctolin in two coleopteran insect species. *Peptides* **22**, 209-217.

Sun, B. D. and Schmidt, J. M. (1997). The structure of the antennal heart of *Aedes aegypti* (Linnaeus). *Can. J. Zool.* **75**, 444-458.

Tang, M., Yuan, W., Bodmer, R., Wu, X. and Ocorr, K. (2014). The role of pygopus in the differentiation of intracardiac valves in *Drosophila*. *Genesis* **52**, 19-28.

Trautwein, M. D., Wiegmann, B. M., Beutel, R., Kjer, K. M. and Yeates, D. K. (2012). Advances in insect phylogeny at the dawn of the postgenomic era. *Annu. Rev. Entomol.* **57**, 449-468.

Tsai, M. T., Chang, F. Y., Lee, C. K., Chi, T. T., Yang, K. M., Lin, L. Y., Wu, J. T. and Yang, C. C. (2011). Observations of cardiac beating behaviors of wild-type and mutant Drosophilae with optical coherence tomography. *J. Biophotonics* **4**, 610-618.

Walker, R. J., Papaioannou, S. and Holden-Dye, L. (2009). A review of FMRFamide- and RFamide-like peptides in metazoa. *Invert. Neurosci.* **9**, 111-153.

Wang, G., Qiu, Y. T., Lu, T., Kwon, H. W., Pitts, R. J., Van Loon, J. J., Takken, W. and Zwiebel, L. J. (2009). Anopheles gambiae TRPA1 is a heat-activated channel expressed in thermosensitive sensilla of female antennae. *Eur. J. Neurosci.* **30**, 967-974.

Wasserthal, L. T. (1980). Oscillating hemolymph circulation in the butterfly *Papilio machaon* L. revealed by contact thermography and photocell measurements. *J. Comp. Physiol.* **139**, 145-163.

Wasserthal, L. T. (1999). Functional morphology of the heart and of a new cephalic pulsatile organ in the blowfly *Calliphora vicina* (Diptera: Calliphoridae) and their roles in hemolymph transport and tracheal ventilation. *Int. J. Insect Morphol. Embryol.* **28**, 111-129.

Wasserthal, L. T. (2007). *Drosophila* flies combine periodic heartbeat reversal with a circulation in the anterior body mediated by a newly discovered anterior pair of ostial valves and 'venous' channels. *J. Exp. Biol.* **210**, 3707-3719.

Wessells, R. J. and Bodmer, R. (2004). Screening assays for heart function mutants in *Drosophila*. *Biotechniques* **37**, 58-60, 62, 64 passim.

Wirkner, C. S., Togel, M. and Pass, G. (2013). The arthropod circulatory system. In *Arthropod Biology and Evolution: Molecules, Development, Morphology* (ed. A. Minelli, G. Boxshall and G. Fusco), pp. 343-391. Heidelberg: Springer.

Zornik, E., Paisley, K. and Nichols, R. (1999). Neural transmitters and a peptide modulate *Drosophila* heart rate. *Peptides* **20**, 45-51.